A 2-dimensional Reduced Oscillator Model with Rational Nonlinearities for p53 Dynamics

Gökhan Demirkıran[1], Güleser Kalaycı Demir[2], and Cüneyt Güzeliş[1]

[1]Department of Electrical and Electronics Engineering, Yaşar University, Bornova, İzmir, 35100, Turkey
gokhan.demirkiran@yasar.edu.tr , cuneyt.guzelis@yasar.edu.tr
[2]Department of Electrical and Electronics Engineering, Dokuz Eylül University, Buca, İzmir, 35160, Turkey
guleser.demir@deu.edu.tr

Abstract

p53 tumour suppressor network plays the key role in DNA damage response of the cell. We present a comprehensive 2-dimensional oscillator model for p53 network dynamics. The model is reduced from the known 17-dimensional two-phase model of p53 network, which shows temporary oscillatory behaviour under DNA damage type of Double Strand Breaks. The introduced oscillator model shows the same qualitative dynamics of two-phase model of p53 network, such as bistability and oscillations, when the parameters are adjusted accordingly. With the help of the identified oscillator in p53 network, we introduce a new oscillator perspective: p53 network has an oscillator in the centre, which other systems in the cell manipulate this oscillator to contribute to cell fate. The introduction of such low dimensional oscillator model will make it possible to study p53 network and the effects of other biological systems in the context of oscillations.

1. Introduction

p53 network is a critical gene regulatory network that is studied thoroughly since the majority of human tumors occur due to the defects in this network [1]. The core gene of this network is called as TP53 or P53, and the product of that gene is the protein p53. p53 network is responsible for avoiding the risks associated with DNA damage that may occur due to various stress types, such as hypoxia, telomere erosion, heat shock, ultraviolet (UV) radiation, and (gamma) Ionizing Radiation (IR) [2]. The understanding of how p53 network responds to these stresses is important since cancer therapies, such as radiotherapy and chemotherapy, use this network to suppress tumour growth via apoptosis (programmed cell death). In this paper, the primary consideration will be p53 network's oscillatory response to stress type of IR that causes Double Strand Breaks (DSBs) in DNA.

The first evidence of p53 network exhibiting oscillatory dynamics has been shown by giving IR to a cell population [3]. In this experiment, p53 concentration performed damped oscillations, which was obtained by averaging over cell population. However, single cell studies have shown that it is actually an oscillation, which looks like damped oscillation due to shifts in synchronicity when averaged over a population of cells [4] [5].

Although several high-dimensional models have been proposed for oscillatory dynamics of p53, the literature lacks of a comprehensive low dimensional (e.g. 2-dimensional) oscillator model for p53 dynamics [6]. The existence of low dimensional models (two or three dimensional) for other known biological oscillators, such as circadian rhythm and neuronal populations, made it possible to study these systems within the instruments of oscillator coupling concept, such as synchronization and entrainment properties. For instance, studying the synchronization in SupraChiasmatic Nucleus (SCN) cells by 2-dimensional phase oscillators, in which all the main ingredients of a circadian rhythm can be embedded, have shown that coupling in SCN provides robustness against noise, period mismatch, genetic perturbations, mutations or external environmental cues [7] [8] [9] [10] [11]. Although potential coupling mechanisms, (e.g. Radiation Induced Bystander Effects [12] [13], circadian rhythm [14]) exist in p53 network, the lack of comprehensive 2-dimensional model for p53 dynamics creates a resistance against studying such effects thoroughly from the oscillator perspective that engineers are very informed about. The aim of this paper is to propose such a low dimensional model that will be used for further studies of p53 dynamics from the oscillator perspective.

This paper is organized as follows. In Section 2, we review the two-phase model in a way that will be helpful for reduction, in Section 3, we introduce the reduced model and give reduction steps.

2. Overview of Two-phase Model

A comprehensive 17-dimensional mathematical model has been proposed in [15], where the p53 network may exhibit one- or two-phase dynamics. Under IR, DSBs occur and repair molecules form a complex with DSBs (DSBCs) to repair DSBs. The number of DSBs can be as high as 500 however there are as low as 20 repair molecules in the cell. Thus, in a full repair activity, i.e. all repair molecules are assigned to a DSB, maximum of 20 DSBCs may exist (See Fig. 1a). When a repair molecule finishes repairing a DSB, it is assigned to another DSB so that all DSBs can be repaired. The number of DSBCs (n_c) is the stimulus of the two-phase model and also in the proposed 2-dimensional oscillator model in this paper.

Two-phase dynamics occur in this way: When DSBs occur, the cell undergoes the first phase where p53 level oscillates. If the amount of damage is not reduced to an acceptable level in a certain amount of time, then cell goes to the second phase raising p53 level to such a high steady state value that it triggers apoptosis mechanism. Or if the damage is fixed in a certain amount of time in the first phase, then the cell does not go to the second phase, and instead p53 level drops to basal steady state. The high and low steady states are features of the bistability characteristics [16] [17] whilst oscillations are the oscillatory behaviour of two-phase model. More concisely, in two-phase model of p53 network, p53 dynamics consists of three modes: low state as in unstressed conditions, oscillations in case of DSBCs, high state in case of excessively long time of DSBCs. One-phase and two-phase

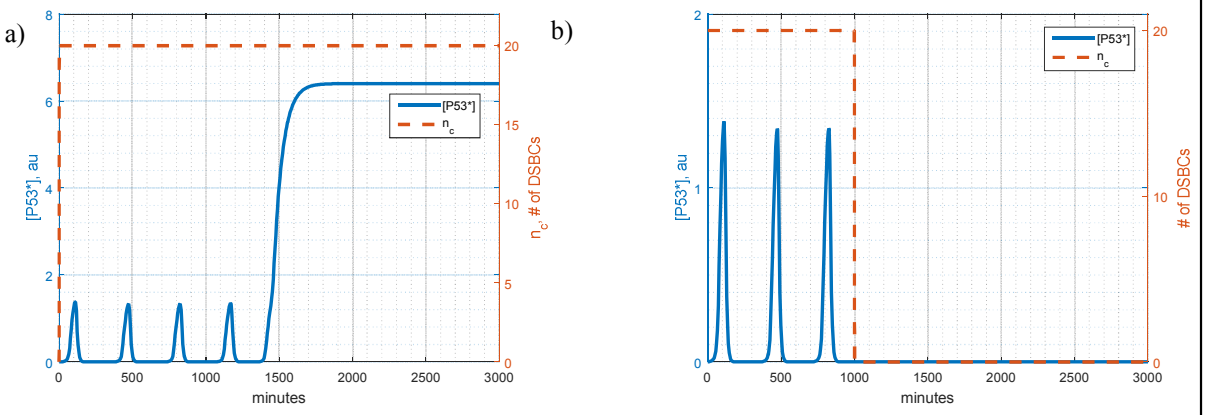

Fig. 1. p53 level exhibiting two-phase dynamics according to the model by [14]. a) Two-phase dynamics is observed if n_c is kept as 20 for a long time (i.e. 1500 minutes). b) The second phase (apoptosis) is not observed, only the first phase is observed if n_c falls to zero before 1500 minutes.

dynamics are demonstrated in Fig. 1. by numerically solving the 17-dimensional model of [15] using "ode45" function of MATLAB software.

The schematic depiction of two-phase model, is given in [15] as a directed graph, which is based on the suppression and enhancing effects of the proteins. Herein, we re-illustrate the two-phase model for a better discussion in view of subsystems in MATLAB/Simulink environment as in Fig. 2, based on differential equations of two-phase model. In the re-illustration, the interrelated molecules are identified as a subsystem to simplify the network. Since herein the diagram is based on the differential equations of two-phase dynamics, coupled variables can easily be seen. This is especially useful when a subsystem's behaviour is intended to be reduced and studied in isolation from its surrounding as will be done in Section 3.

The identified subsystems are ATM sensor subsystem, Wip1 subsystem, Mdm2 subsystem, P53DINP1 subsystem, PTEN subsystem, caspase subsystem and p21 subsystem. Three feedback loops exist in the model as identified in [15] and can be seen from Fig. 2: 1) ATM-p53-Wip1 feedback loop, 2) p53-PTEN-Akt-Mdm2 feedback loop, and 3) p53-Mdm2 feedback loop.

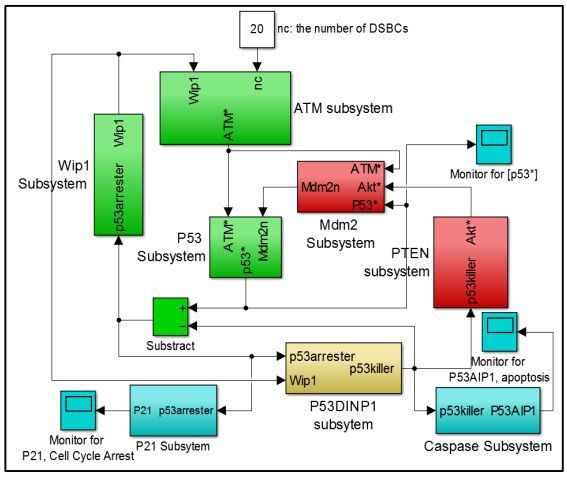

Fig. 2. Representation of 17-dimensional two-phase model with subsystems in Matlab/Simulink.

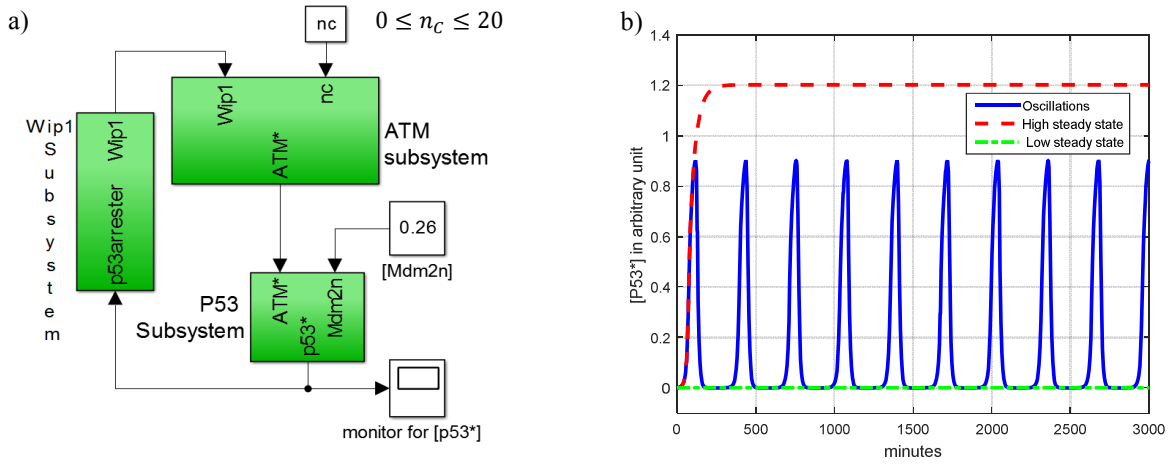

Fig. 3. a) Matlab/Simulink representation of the isolated 6-dimensional core oscillator subsystem of the two-phase dynamics. **b)** Demonstration of three different modes by 6-dimensional core oscillator subsystem defined in Table 1.

It was shown by wet lab experiments that ATM-p53-Wip1 feedback loop (Wip1 feedback loop) is indispensable for oscillations [18]. In the two-phase model, Wip1 feedback loop is essential for oscillations in the first phase, while p53-PTEN-Akt-Mdm2 feedback loop (PTEN feedback loop) becomes active in the second phase [15]. In addition, p53-Mdm2 feedback loop is claimed to be for fine-tuning the period of oscillations in two-phase model [15]. Thus, focusing on the oscillations in the first phase, we isolate the PTEN feedback loop and p53-Mdm2 feedback loop, such that there is only Wip1 feedback loop which is essential for oscillations. The passed variable $Mdm2_n$ from discarded subsystems are assumed as constant equal to its initial value given in [15] (See Fig. 3a). Also as can be seen in Fig. 2., p21 and caspase subsystem do not provide any feedback signal to the p53 network, so their dynamics are ignored (See Fig. 3a).

The resulting isolated system in two-phase model is 6-dimensional as shown in Table-1 and depicted in Fig. 3a. Next, we show that this resulting set of equations is capable of replicating three modes of p53 dynamics, namely low state, oscillations, and high state by manipulating the parameters, n_c, $[p53Arrester]$ and $[p53killer]$. Note that $[p53^*]$ (active p53 concentration) is a variable of 6-dimensional oscillator model and however $[p53Arrester]$ and $[p53killer]$ have become parameters controlled by other subsystems which we discarded. Thus, by appropriately manipulating these parameters, we will show in the sequel that 6-dimensional isolated subsystem is capable of exhibiting bistability and oscillations as 17-dimensional two-phase model does.

When n_c is 0, modelling unstressed case, [p53] level stays at low (See Fig. 3b for different p53 dynamics). When n_c is set to 20 indicating a high DSBC activity, then [p53*] level starts to oscillate. When n_c is zero and the number of $[p53Arrester] = 0$, then [p53*] level goes to high equilibrium state. It must be noted that, in the high equilibrium case of 6-dimensional model, the high level is not as high as in Fig. 1a, where we numerically solved the whole 17-dimensional model. The reason is discarding of PTEN feedback loop whose function is to shift the high equilibrium to higher levels in two-phase model. Thus, we demonstrated that 6-dimensional model exhibits the same qualitative behaviours as 17-dimensional two-phase model.

Since herein we are looking for the core subsystem responsible for qualitative dynamics, the effect of other subsystems in the network is omitted. Thus, we introduce a modular perspective to p53 network. In this modular perspective, an isolated oscillator is at the centre of the p53 network and other subsystems influence this oscillator by influencing various parameters of the oscillator. The other rationale for isolation of 6-dimensional subsystem is that although the biological function of Wip1 feedback loop is well-documented, the biological function of other loops in two-phase model is not well-documented. For instance, it is not known whether PTEN feedback loop increase the high equilibrium state in the second phase, although it is known that it contributes to apoptosis. However, authors of [15] find it logical to model this behaviour of PTEN as increase in the high equilibrium state. By discarding these not so well-documented loops, we keep the core well-documented biological subsystem of two-phase model for reduction. It must be noted that mathematical models in systems biology are never complete. The models are as good as they can provide new predictions and new hypothesizes about the working of the system, which can be tested in wet lab settings.

Table 1. 6-dimensional core oscillator subsystem of two-phase dynamics (for meaning of parameters and their values, please refer to [16])

Equation number	Equations
1	$\frac{d[ATM_2]}{dt} = 0.5k_{dim}[\boldsymbol{ATM}]^2 - k_{undim}[ATM_2]$
2	$\frac{d[ATM^*]}{dt} = k_{acatm}\frac{n_c}{n_c + j_{nc}} * [ATM^*] * \frac{[ATM]}{([ATM] + j_{acatm})} - k_{deatm}(1 + [Wip1]) * \frac{[ATM^*]}{([ATM^*] + j_{deatm})}$
3	$\frac{d[p53^*]}{dt} = k_{acp53}[p53] - k_{dep53}[p53^*] - k_{dp53s}[Mdm2_n]\frac{[p53^*]}{j_{1p53n} + [p53^*]}$
4	$\frac{d[p53]}{dt} = k_{sp53} - k_{dp53n}[p53] - k_{dp53}[Mdm2_n]\frac{[p53]}{j_{1p53n} + [p53]} - k_{acp53}[p53] + k_{dep53}[p53^*]$
5	$\frac{d[Wip1]}{dt} = k_{swip10} + k_{swip1}\frac{[p53Arrester]^3}{({j_{swip1}}^3 + [p53Arrester]^3)} - k_{dp21}[Wip1]$
6	$\frac{d[Mdm2_n]}{dt} = k_i[Mdm2_{cp}] - k_0[Mdm2_n] - k_{dmdm2n}[Mdm2_n]$
7	$[ATM] = ATM_{tot} - 2[ATM_2] - [ATM^*]$; $k_{acp53} = k_{acp531}\frac{[ATM^*]}{([ATM^*] + j_{atm})}$; $k_{dmdm2n} = k_{dmdm2n0} + k_{dmdm2n1}\frac{[ATM^*]}{([ATM^*] + j_{atm})}$
8	$[p53^*] = [p53Arrester] + [p53killer]$

3. Reduction to 2-dimension

In this section, we present a comprehensive 2-dimensional oscillator model for p53 network as defined in Table 2. The steps of reduction are given as in the sequel so that other researchers can follow the steps and change them as they like to produce their own parametric 2-dimensional model to fit in a context. The proposed 2-dimensional oscillator model described by the state equations with rational right-hand side is capable of showing three different qualitative modes of p53 dynamics relevant to cell fate outcomes: low equilibrium state, oscillation, and high equilibrium state. When n_c is set to 20, p53 level ([p53*]) starts to oscillate. After 750 minutes passed, [p53arrester] is made zero in the solver algorithm to indicate that all p53* consists of p53killer now (Refer Equation 3 of Table 2). In this case, [p53*] value goes to a high steady state as shown in Fig. 4.

In the 2-D model, [ATM*] and [Wip1] are the variables of the oscillator while [p53*] is described with an algebraic equation (See Equation 3 of Table 1). [p53*] equation is inversely correlated with its inhibitor [$Mdm2_n$], it is directly proportional to its activator [ATM*] (i.e. phosphorylated ATM). Therefore, the ATM dynamics reflects on [p53*]. [p53*] oscillates whenever [ATM*] oscillates. When [ATM*] is in high or low steady state, [p53*] is at a high or low level, respectively. This reduction is also consistent with the experimental observation that ATM is the main upstream signal of p53 dynamics and p53 pulses originate from recurrent initiation of ATM [18]. The number of DSBCs (i.e. n_c) is an external stimulus that starts the oscillations.

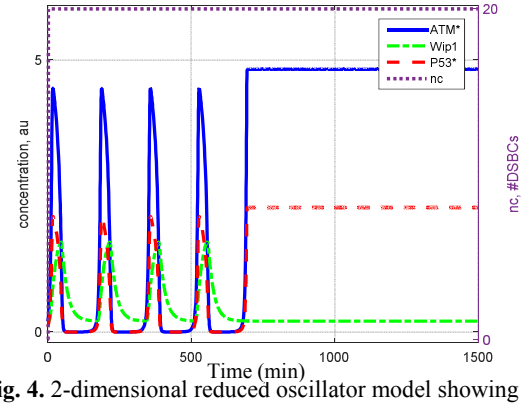

Fig. 4. 2-dimensional reduced oscillator model showing two-phase dynamics.

Reduction Steps:

ATM sensor subsystem consists of two differential equations, as shown by the equations for $\frac{d[ATM_2]}{dt}$ and $\frac{d[ATM^*]}{dt}$ in Table 1. Since ATM* is an active protein that effects downstream modules, we keep ATM* as a variable and eliminate ATM_2 by quasi-steady state assumption. Thus, by assuming $\frac{d[ATM_2]}{dt} = 0$, then we can express $[ATM_2]$ as algebraic equation below.

$$[ATM_2] = \quad 0.5 * \frac{k_{dim}}{k_{undim}} * [ATM]^2$$

Then, putting $[ATM_2]$ expression into $[ATM] = ATM_{tot} - 2[ATM_2] - [ATM^*]$ to obtain:

$$[ATM] = ATM_{tot} - 2 * 0.5 \frac{k_{dim}}{k_{undim}} [ATM]^2 - [ATM^*]$$

$$[ATM] + 2 * 0.5 * \frac{k_{dim}}{k_{undim}} * [ATM]^2 = ATM_{tot} - [ATM^*]$$

where $k_{dim} = 10$ and $k_{undim} = 1$. Replacing the values of k_{dim} and k_{undim} and after a few arrangements in the equation, we obtain [ATM] as:

$$[ATM] + 10[ATM]^2 = ATM_{tot} - [ATM^*] \qquad (1)$$

$$10[ATM]^2 \cong ATM_{tot} - [ATM^*] \qquad (2)$$

$$[ATM] = \sqrt{0.1(ATM_{tot} - [ATM^*])} \qquad (3)$$

Putting Equation (3) in appropriate places in the right-hand side of the equtaion for $\frac{d[ATM^*]}{dt}$ in Table 1, then we obtain the $\frac{d[ATM^*]}{dt}$ equation in Table 2:

Now we eliminate p53 subsystem completely writing it as an algebraic equation. p53 subsystem equations are the Equations 3 and 4 of Table 1. Since p53* is the active protein, we want to write [p53*] as an algebraic equation.

The rational term $\frac{[p53]}{j_{1p53n}+[p53]}$ in $\frac{d[p53]}{dt}$ of Table 1 makes it hard to write [p53] as an algebraic expression. Thus, we linearize this rational term. j_{1p53n} is 0.1 and [p53] changes between 0.4 and 1.4 in the oscillation phase. Thus, an appropriate linearization would be:

$$\frac{[p53]}{0.1 + [p53]} \cong 0.1333 * [P53] + 0.7467$$

Putting this linearized expression into the equation for $\frac{d[p53]}{dt}$ of Table 1 and then equating $\frac{d[p53]}{dt}$ to zero, [p53] becomes a function of [$Mdm2_n$] parameter and [$p53^*$] variable as shown in the below equation.

$$[p53_{linearized}] = \frac{(k_{sp53} - k_{dp53}\,[Mdm2n]\ 0.7467 + k_{dep53}\,[P53^*])}{k_{dp53n} + k_{dp53}\,[Mdm2n]\ 0.1333 + k_{acp53}\,(ATM^*)}$$

Table 2. The introduced 2-dimensional oscillator model for p53 network.

Equation number	Equations
1	$\frac{d[ATM^*]}{dt} = k_{acatm}\ \frac{n_c}{(n_c + jn_c)}\,[ATM^*]\ \frac{\sqrt{0.1*(ATM_{tot}-[ATM^*])}}{(\sqrt{0.1*(ATM_{tot}-[ATM^*])} + jacatm)} - k_{deatm}\ \frac{(1+[Wip1])[ATM^*]}{([ATM^*]+j_{deatm})}$
2	$\frac{d[Wip1]}{dt} = k_{swip10} + k_{swip1}\ \frac{[p53Arrester]^3}{(j_{swip1}{}^3+[p53Arrester]^3)} - k_{dwip1}[Wip1]$
3	$[p53^*] = [p53arrester] + [p53killer] = [ATM^*](1.5 - 3.947[\,Mdm2_n\,])$

Replacing [p53] in $\frac{d[p53^*]}{dt}$ with $p53_{linearized}$, $\frac{d[p53^*]}{dt}$ becomes:

$$\frac{d[P53^*]}{dt} = k_{acp53}\,(ATM^*)[p53_{linearized}] - k_{dep53}\,[P53^*] - k_{dp53s}\,[Mdm2_n]\frac{[P53^*]}{(j_{1p53n} + [P53^*])}$$

To solve $[P53^*]$ as a compact algebraic function of the resting variables, we need to make quasi-steady state assumption and linearize the rational term $\frac{[P53^*]}{(j_{1p53n}+[P53^*])}$:

$$\frac{[p53^*]}{0.1 + [p53^*]} \cong 0.667 * [p53^*]$$

Replacing the linearized term, $\frac{d[p53^*]}{dt}$ becomes:

$$\frac{d[p53^*]}{dt} = k_{acp53}\,(ATM^*)[p53_{linearized}] - k_{dep53}\,[p53^*] - k_{dp53s}\,[Mdm2_n]0.667[p53^*]$$

Equating $\frac{d[p53^*]}{dt} = 0$ and after several simplifications linearized [p53*] equation is found as:

$$[p53^*] = [ATM^*](1.5 - 3.947 * [Mdm2_n])$$

So far, we have obtained [ATM*] dynamics as one dimensional differential as in Equation 1 of Table 2, [p53*] as an algebraic equation in Equation 3 of Table 1. We keep the Wip1 dynamics as in the 17-dimensional model of two-phase dynamics by [15] without changing it, which is the Equation 2 of Table 2.

6. Conclusions

Herein we presented a 2-dimensional oscillator model to be used in p53 network research. The introduced 2-dimensional oscillator can be used as a module for p53-related larger networks as new subsystems of p53 network or other networks that effect p53 network are discovered. One candidate for such a network is circadian network, which is known to be a biological oscillator that positively effects p53 network. Since circadian is an oscillator and p53 dynamics is also an oscillator (as we have shown here), it is better to study the effect of these systems to each other in the context of oscillator coupling. For such a study, these two systems must be kept as two separated oscillator models capable of signalling each other. The introduced 2-dimensional model will serve in this direction for further research.

References

[1] S. Jin and A. J. Levine, "The p53 functional circuit," *Journal of cell science,* pp. 4139-4140, 2001.

[2] F. Murray-Zmijewski, E. A. Slee and X. Lu, "A complex barcode underlies the heterogeneous response of p53 to stress," *Nature reviews Molecular cell biology,* pp. 702-712, 2008.

[3] Bar-Or, R. Lev, R. Maya, L. A. Segel, U. Alon, A. J. Levine and a. M. Oren, "Generation of oscillations by the p53-Mdm2 feedback loop: a theoretical and experimental study," *Proceedings of the National Academy of Sciences,* pp. 11250-11255, 2000.

[4] G. Lahav, N. Rosenfeld, A. Sigal, N. Geva-Zatorsky, A. J. Levine, M. B. Elowitz and U. Alon, "Dynamics of the p53-Mdm2 feedback loop in individual cells," *Nature Genetics,* pp. 147-150, 2004.

[5] E. Batchelor, A. Loewer and G. Lahav, "The ups and downs of p53: understanding protein dynamics in single cells," *Nature Reviews Cancer,* pp. 371-377, 2009.

[6] T. Sun and J. Cui, "Dynamics of P53 in response to DNA damage: Mathematical modeling and perspective," *Progress in biophysics and molecular biology ,* pp. 175-182, 2015.

[7] C. Ko, Y. Yamada, D. Welsh, E. Buhr, A. Liu, E. Zhang, M. Ralph, S. Kay, D. Forger and J. Takahashi, "Emergence of noise-induced oscillations in the central circadian pacemaker," *PLoS biology,* p. p.e1000513, 2010.

[8] Y. Hasegawa and M. Arita., "Enhanced entrainability of genetic oscillators by period mismatch," *Journal of The Royal Society Interface,* p. 20121020, 2013.

[9] A. C. Liu, D. K. Welsh, C. H. Ko, H. G. Tran, E. E. Zhang, A. A. Priest, E. Buhr, O. Singer, K. Meeker, I. Verma and F. J. Doyle, "Intercellular coupling confers robustness against mutations in the SCN circadian clock network," *Cell,* pp. 605-616, 2007.

[10] C. Gu, X. Liang, H. Yang and J. H. Rohling, "Heterogeneity induces rhythms of weakly coupled circadian neurons," *Scientific reports,* p. 6, 2016.

[11] A. Granada and H. Herzel, "How to achieve fast entrainment? The timescale to synchronization," *PLoS One,* p. p.e7057, 2009.

[12] J. B. Little, "Cellular radiation effects and the bystander response.," *utation Research/Fundamental and Molecular Mechanisms of Mutagenesis,* pp. 113-118, 2006.

[13] M. He, M. Zhao, B. Shen, K. Prise and C. Shao, "Radiation-induced intercellular signaling mediated by cytochrome-c via a p53-dependent pathway in hepatoma cells," *Oncogene,* pp. 1947-1955, 2011.

[14] A. Sancar, L. A. Lindsey-Boltz, T. H. Kang, J. T. Reardon, J. H. Lee and N. Ozturk, "Circadian clock control of the cellular response to DNA damage," *FEBS letters,* pp. 2618-2625, 2010.

[15] X.-P. Zhang, F. Liu and W. Wang, "Two-phase dynamics of p53 in the DNA damage response," *Proceedings of the National Academy of Sciences,* pp. 8990-8995, 2011.

[16] N. Avcu, N. Pekergin, F. Pekergin and C. Guzelis, "Aggregation for Computing Multi-Modal Stationary Distributions in 1-D Gene Regulatory Networks," *IEEE/ACM Transactions on Computational Biology and Bioinformatics,* 2017(to be published).

[17] N. Avcu, H. Alyürük, G. K. Demir, F. Pekergin, L. Cavas and C. Güzeliş., "Determining the bistability parameter ranges of artificially induced lac operon using the root locus method.," *Computers in biology and medicine,* pp. 75-91, 2015.

[18] E. Batchelor, C. S. Mock, I. Bhan, A. Loewer and G. Lahav, "Recurrent initiation: a mechanism for triggering p53 pulses in response to DNA damage," *Molecular cell,* pp. 277-289, 2008.